REPORT DOCUMENTATION PAGE

AFRL-SR-AR-TR-04-

0558

1. REPORT DATE (DD-MM-YYYY)	2. REPORT TYPE	3. DATES COVERED (From - To)
30-04-2004	FINAL TECHNICAL	23 Sep 1998 - 31 Oct 2003

4. TITLE AND SUBTITLE

AVIA: Adaptive Virtual Aerosurface

5a. CONTRACT NUMBER

5b. GRANT NUMBER
F49620-98-1-0503

5c. PROGRAM ELEMENT NUMBER

6. AUTHOR(S)
D. Parekh, A. Glezer, M. Allen, T. Crittenden, E. Birdsell, and R. Funk

5d. PROJECT NUMBER

5e. TASK NUMBER

5f. WORK UNIT NUMBER

7. PERFORMING ORGANIZATION NAME(S) AND ADDRESS(ES)

Georgia Tech Applied Research Corporation (GTARC)
400 10th St., NW
Atlanta, GA 30332

Boeing Company, P. O. Box 516
St. Louis, MO 63166-0516

Metacomp Technologies
650 Hampshire Rd., Suite 200
Westlake Village, CA 91361

8. PERFORMING ORGANIZATION REPORT NUMBER

9. SPONSORING / MONITORING AGENCY NAME(S) AND ADDRESS(ES)
AFOSR
4015 Wilson Blvd., Rm 713
Arlington, VA 22203-1954

10. SPONSOR/MONITOR'S ACRONYM(S)
AFOSR-Air Force Office of Scientific Research

11. SPONSOR/MONITOR'S REPORT NUMBER(S)

12. DISTRIBUTION / AVAILABILITY STATEMENT

Distribution Statement "A" (Approved for Public Release, Distribution Unlimited).

13. SUPPLEMENTARY NOTES

20041109 012

14. ABSTRACT

One can change the effective shape of a surface without any change in its physical moldlines through the transient injection of momentum to control unsteady flow phenomena, such as separation. This research program consists of a system level evaluation of the potential benefits and costs of active flow control as applied to UAVs for separation control, development of innovative actuator concepts, and proof-of-concept experiments showing aerodynamic effectiveness. System-level benefits include increased gust margin, reduced takeoff field length, increased payload capacity, and greater maneuverability. Actuator research has resulted in two major innovations: the use of pulsed/modulated waveforms to increase the effectiveness of synthetic jet actuators and the development of compact, high power, combustion-driven actuator modules. The general performance of the combustion actuators are characterized in isolation, embedded in cross-flows up to M=0.7, and integrated on a two-dimensional wing model. In addition, since conventional machining would not be suitable for low-cost, large volume production, a simpler, MEMS-based, batch fabrication

15. SUBJECT TERMS
active flow control, synthetic jet, actuators, separation control

16. SECURITY CLASSIFICATION OF:			17. LIMITATION OF ABSTRACT	18. NUMBER OF PAGES	19a. NAME OF RESPONSIBLE PERSON
a. REPORT	b. ABSTRACT	c. THIS PAGE			Dr. David E. Parekh
UNCLASSIFIED	UNCLASSIFIED	UNCLASSIFIED	NONE	102	19b. TELEPHONE NUMBER (include area code) (404)894-3369

AVIA: Adaptive Virtual Aerosurface

D. Parekh, A. Glezer, M. Allen, T. Crittenden, E. Birdsell, and R. Funk
Georgia Institute of Technology, Atlanta, GA 30332

30 April 2004
Final Technical Report
Grant F49620-98-1-0503

Prepared for:
Dr. Tom Beutner
UNITED STATES AIR FORCE
Air Force Office of Scientific Research
Arlington, VA 22203

Preface

This research was sponsored through a grant from the Air Force Office of Scientific Research (AFOSR). Funding for this work was provided by the MicroAdaptive Flow Control Program (MAFC) of the Defense Advance Research Project Agency (DARPA). The AFOSR technical monitor is Dr. Tom Beutner; the DARPA MAFC program manager is Dr. Steve Walker. This project was initiated in September 1998 and continued through multiple phases, concluding in October 2003.

A team of researchers from the Georgia Institute of Technology, the Boeing Company, and Metacomp Technologies partnered together to conduct this work. Key participants from these institutions are noted in the Acknowledgements section of this report.

Executive Summary

Traditionally, air vehicles have achieved aerodynamic control through movement of control surfaces. By producing an unsteady flux of momentum through an aerodynamic surface, one can alter the external flow field and associated surface pressure distribution. In this way, modifications of forces and moments on a surface can be accomplished without any physical change in a moldline or movement of control surfaces. Hence, this flow control concept is known as Adaptive Virtual Aerosurface (AVIA).

The objective of the AVIA program is to enable enhanced aerodynamic performance extending into the post-stall regime. This provides significant mission-specific benefits such as increased payload capacity and improved gust margin. The specific goals for this program concern the development of a combustion-based actuator for greater control authority and an increase in the useful angle-of-attack range. The research was conducted in two phases that included a system level evaluation of the potential benefits and costs of active flow control as applied to UAVs for separation control, development of innovative actuator concepts, and proof-of-concept experiments and computations showing aerodynamic effectiveness.

The key technical results of this program are documented in this report, a PhD dissertation, and a set of published papers. System-level benefits include increased gust margin, reduced takeoff field length, increased payload capacity, and greater maneuverability. The actuator research has resulted in two major innovations: the use of pulsed/modulated waveforms to increase the effectiveness of synthetic jet actuators and the development of compact, high power, combustion-driven actuator modules. The general performance of the combustion actuators are characterized on a two-dimensional wing model, in which case flow attachment was maintained for more than 10 degrees beyond the nominal stall margin. In addition, a MEMS-based, batch fabrication approach, simpler than conventional machining, was developed for manufacturing these actuator modules. The AVIA concept shows tremendous promise for achieving significant, mission-specific, aerodynamic benefits and is ready for consideration for specific applications through subsequent technology development and transition programs.

TABLE of CONTENTS

1. Introduction

1.1 AVIA Concept

Traditionally, air vehicles have achieved aerodynamic control through movement of control surfaces. Recent fluid dynamics research has provided an alternate path. Through producing an unsteady flux of momentum on an aerodynamic surface, one can alter the flow field and associated surface pressure distribution. In this way, modifications of forces and moments on an air vehicle can be accomplished without any physical change in a moldline or movement of control surfaces. Adaptive Virtual Aerosurface (AVIA) is a term coined for the concept of using flow interactions rather than altering physical shape for aerodynamic control.

1.2 Program Overview

The objective of the AVIA program is to enable enhanced aerodynamic performance extending into the post-stall regime. This provides significant mission-specific benefits such as increased payload capacity and improved gust margin. The specific goals for this program concern the development of a combustion-based actuator for greater control authority and an increase in the useful angle-of-attack range.

The research effort was conducted in two phases. The initial four-month Phase I effort focused on system studies of generic unmanned air vehicles (UAVs) to determine the potential benefits of this technology, specification of a suitable closed-loop control approach based on adaptive neural net methodologies (later expanded by Idan *et al.* [2003]), and a proof-of-concept experiment of piezoelectric synthetic jet flow control on a scaled semi-span wind tunnel model. The initial year of Phase II continued development of the piezoelectric synthetic jet based approach, expanding the suite of scaled wind tunnel experiments, applying time-accurate CFD (Computational Fluid Dynamics) simulations to model the aerodynamic response (see Parekh, Palaniswamy, and Goldberg [2002]), and developing flight-ready power electronics. In the second and remaining years of the Phase II effort, the program was refocused specifically on developing a new concept for high power actuation, based on pulse micro-combustion modules. In addition, the system studies were carried out in greater detail with a specific focus on the X-

45A vehicle and the UCAV (Unmanned Combat Air Vehicle) mission. During the Phase II program, the scope of the effort consisted of four primary components: system analysis, actuator development, actuator subsystem integration, and aerodynamic characterization.

With regard to the system studies, during Phase I, an analysis of a generic set of UAVs, spanning the range from hand-launched to much larger tactical UAVs was conducted. Depending on the platform, significant improvements in turning radius, stall margin, and flight controls weight reduction were estimated to be achievable through application of active flow control. A summary of some of the key results of this generic study are included in the AVIA overview by Parekh & Glezer [2000]. During Phase II, a more specific system study of the potential benefit of AVIA for the DARPA/Air Force UCAV (Unmanned Combat Air Vehicle) was conducted by Boeing as part of this program. The specific platform considered in the study was the X-45A demonstration vehicle. Major benefits were identified in both low-speed and high-speed regimes. Major benefits include significant increases in payload capacity (or reduction in take-off field length), improved gust margin, and improved maneuverability. Specific results are program sensitive and are not included here.

1.3 Report Overview

This report provides a general overview of key technical results and a detailed description of the combustion based actuator concept. Section 2 provides a technical overview of aerodynamic control using a combustion based actuator array embedded in a two-dimensional wing in a low-speed flow. Time sequenced PIV (Particle Image Velocimetry) measurements detail the transient response of the separated flow to the actuator impulse. In Section 3, the potential need for low-cost, batch fabrication of large numbers of these combustion arrays is addressed through a MEMS-based (Micro-Electro-Mechanical Systems) approach developed as part of this research program. Key technical achievements are summarized in Section 4, and an extensive characterization of the novel combustion actuator is included in the Appendix. The Appendix consists of an excerpt from the PhD thesis by Crittenden [2003], which was funded by this project.

2. Aerodynamic Control via Combustion Actuators

2.1 Background

Control of flow separation over wings at moderate to high angles of attack for increased aerodynamic performance has been the goal of many studies. Numerous methods of controlling separating flows have been investigated and employed for many years. Passive methods like vortex generators have been used for reattaching flow over control surfaces on production aircraft. These passive methods have the undesired effect of slightly reduced performance at lower angles of attack. More recently, active flow control methods have been investigated and demonstrated including pulsed blowing and synthetic jets. Pulsed blowing uses coupling with and amplification of global flow instabilities to energize and reattach separated flows. These methods typically used reduced frequencies of O(1) such that the excitation period scales with the time of flight over the length of the reattached flow. Synthetic jets have been demonstrated to modify the apparent aerodynamic shape of a body with actuation reduced frequencies of O(1-100). A detailed review of the fundamentals of synthetic jets is provided by Glezer and Amitay (2002).

Observations during the initial year of this effort regarding the transient nature of flow separation led to the development of square-wave-modulated sinusoidal excitation as a more effective excitation waveform than a continuous sine wave. This approach also requires less power than pure sine wave excitation since the duty cycle is 50% or less. Full-scale evaluation of the performance of synthetic jets and this modulation approach on a flying wing UAV is discussed by Amitay *et al.* (2003) and Parekh *et al.* (2003).

The limitation of most flow control methods typically is actuator power, particularly as the concept is scaled to higher speeds. The need for greater control authority motivated this work's focus on the development and testing of a new class of actuators: micro-combustion-driven modules. The new class of actuators developed under this program has the benefit of high

momentum due to the energy release of the combustion process (Crittenden *et al.* [2001]). There is an order of magnitude increase in momentum coefficient as compared to the steady jet of fuel/air mix through the same orifice. In contrast to most other flow control actuators which use sinusoidal or possibly square wave actuation, the combustion actuator is impulsive. The width of the impulse is controlled by the geometry of the actuator and the fuel used. It remains substantially the same shape for a range of actuation frequencies.

The Appendix, which consists of an excerpt from the PhD thesis by Crittenden [2003], provides a detailed description of the combustion-based actuators pioneered in this study. Time-dependent pressure measurements characterize the performance of these devices as a function of geometry, fuel type, air/fuel ratio, and other key parameters. Instantaneous time-sequenced photography of the combustion chamber provides insight regarding the combustion dynamics and internal flow patterns. The nature of the fluidic interaction of these devices with an external flow is summarized below and is discussed by Crittenden [2001, 2003] and Funk *et al.* [2002].

2.2 Single-Actuator in Crossflow

A single combustion actuator was tested in a high-speed crossflow. A single combustion actuator with a 1-cc volume and 1.25-mm-diameter orifice was placed in the wall of a high-speed indraft wind tunnel. Figure 1 shows schlieren imagery of the actuation peak at M=0.4 and M=0.7. The peak penetration distance of the jet was 11 diameters at M=0.4 and 6 diameters at M=0.7. The penetration of the fuel/air flow with no combustion at these speeds was much less than 1 diameter. These images demonstrate the momentum amplification achieved using combustion.

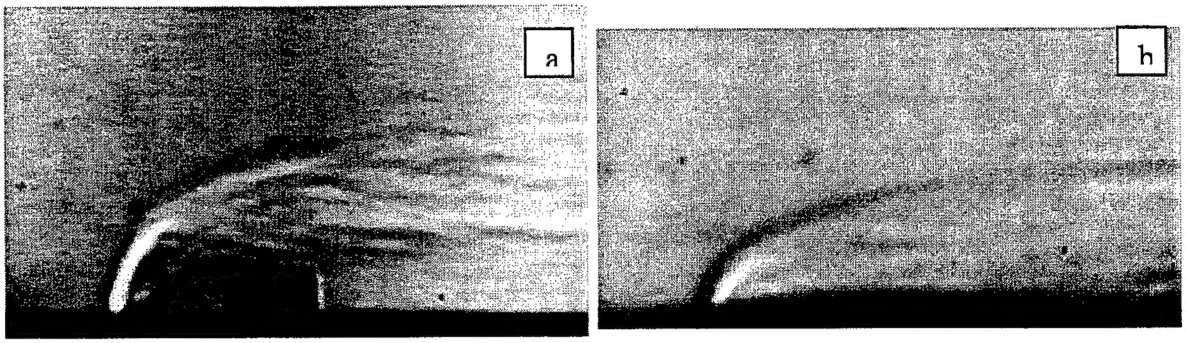

Figure 1. Schlieren images for actuator at peak pressure in a) M=0.4 and b) M=0.7 crossflows. (Note: bolt head in image a is outside the plane of the orifice.)

2.3 Control of Flow Separation

An application of multiple combustion actuators experimentally demonstrated was the control of separation over a wing at 24 degrees angle of attack. A section of the wing constrained by fences had actuators installed blowing normal to the wing surface at the leading edge. Figure 2 shows the separated flow over the wing. The steady fuel/air supply to the actuator did not substantially change the flow. The reduced frequency of actuation was varied from 0.055 to 0.82. Low frequency actuation induced a transient reattachment. Flow was reattached over the wing surface for a time period corresponding to the time of flight of the vortex shed from the leading edge of the wing. As the reduced frequency approached one, the flow stayed attached throughout the actuation cycle. Figure 3 illustrates this reattachment cycle for a reduced frequency of 0.27. The actuator pulse generates a vortex at the leading edge which convects over the upper surface of the wing causing transient reattachment of the flow after its passage. For this reduced frequency the flow then

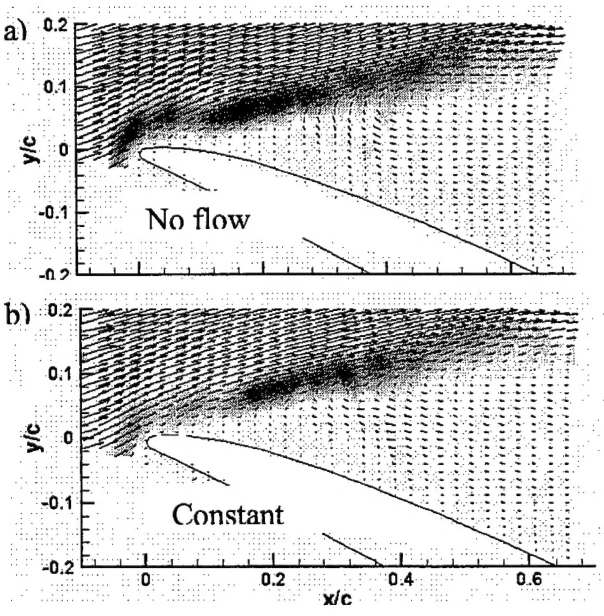

Figure 2. Velocity/vorticity plots for the flowfield with no pulse actuation Re_c = 360,000: a) no flow through actuation slot; b) fuel/air mix flowing through actuation slot.

separates again near the end of the cycle.

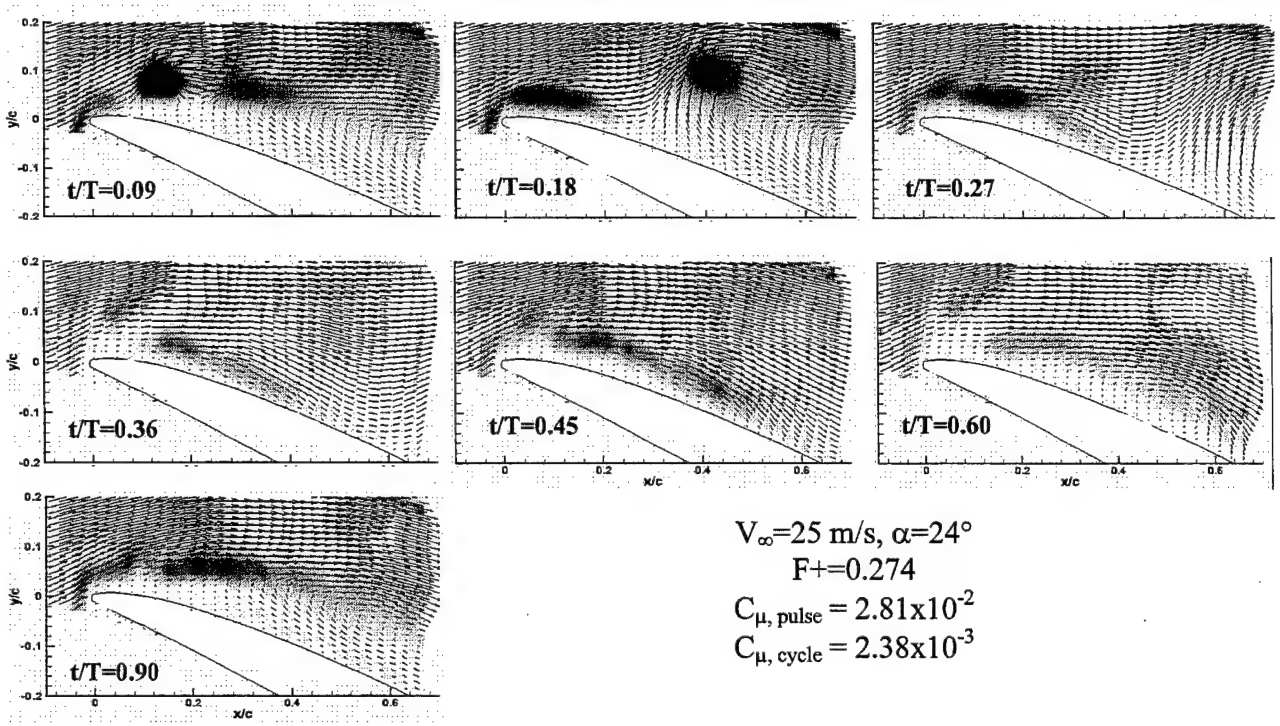

Figure 3. Actuation at $F^+ = 0.274$, Re_c =360,000.

One of the important attributes of the present actuation approach is that it relies on transient actuation to affect the flow and induce attachment. The impulsive nature of the pulse from the combustion actuator and the high momentum of the jet provide transient control at varying actuator frequencies. The momentum of the pulse is controlled by the combustion process (the reaction time is fixed for a particular volume) and not by the actuation frequency. So the initial effect of each pulse is independent of the frequency of actuation. This was verified by running the actuators at a very low frequency (F+ ~ 0.05) and analyzing the resulting flow. The flow exhibited the same shed vortex from the leading edge. Figure 4 is a flow visualization sequence of the initial evolution of the shed vortex. The times on the figure denote the time elapsed since the ignition of the combustion actuator. The vortex is observed forming between 2 and 3 ms after ignition. It then translates along the shear layer and reattaches the flow over the surface. As the reduced frequency is increased the shed vortex remains closer to the wing surface.

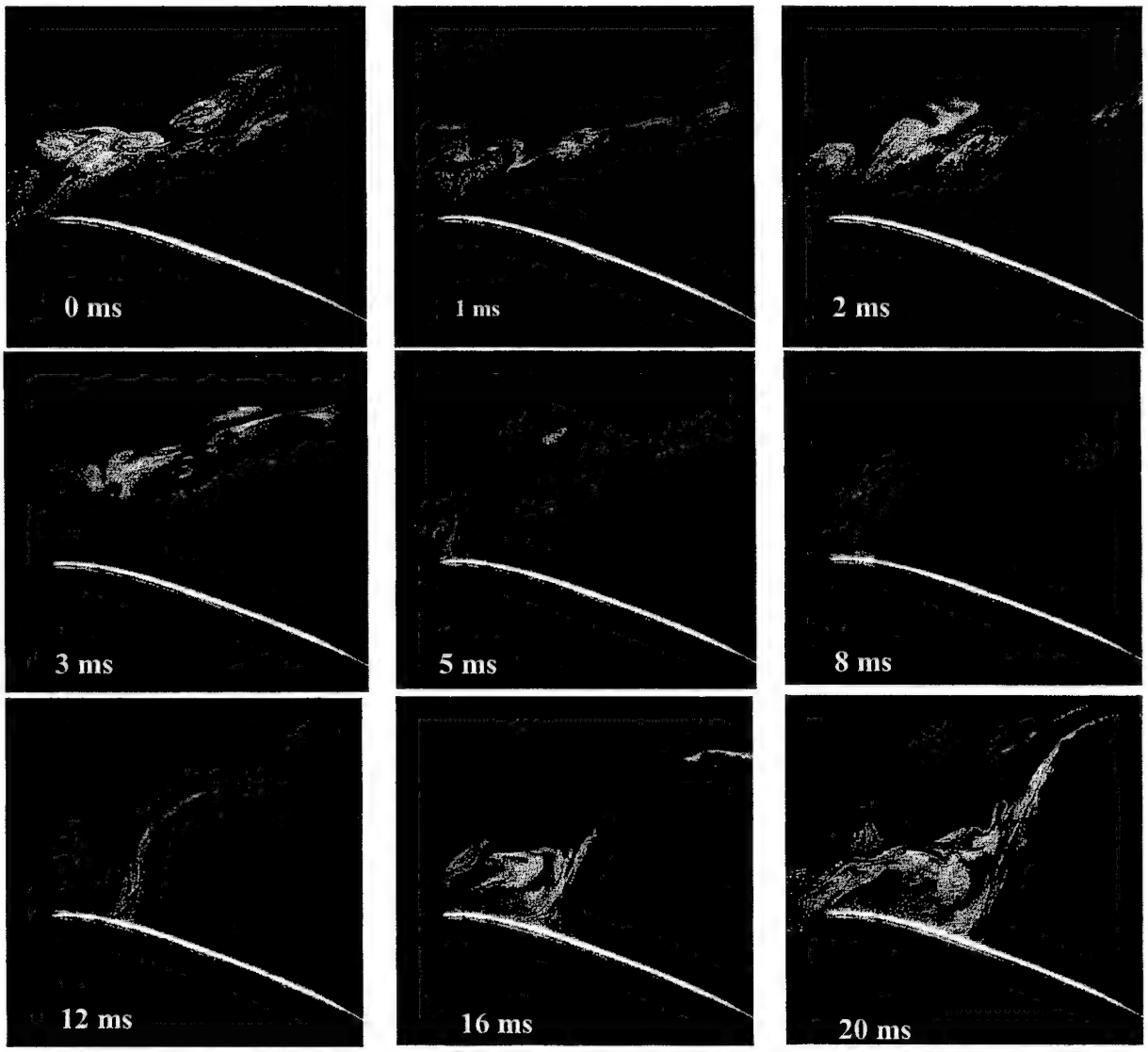

Figure 4. Transient sequence, $F^+ = 0.055$, $\alpha = 24°$, $V_\infty = 12.5$ m/s.

It is observed that F^+ has little effect on the transient process of separated flow reattaching to the airfoil surface. It does have a small effect on the shed vortex convection velocity, possibly through the change in vortex spacing associated with the change in time interval between pulses. F^+ is more important as a governing parameter in the dynamics of flow separating from (rather than reattaching to) the surface. If F^+ is too low, actuation reattaches the flow, but the flow separates again before the next pulse occurs. However, if F^+ is high enough, the flow never has an opportunity to separate from the airfoil. These observations are consistent with the

reattachment transients discussed by Amitay and Glezer (2003) in their study of the dynamics of flow reattachment initiated by synthetic jet actuators.

The high power of these pulse combustion actuators opens many new possibilities for active flow control. At transonic speeds, computational studies conducted as part of the current program have suggested that these actuators would be effective in controlling shock-induced separation. To explore this concept experimentally, a two-dimensional, transonic, stainless steel airfoil was designed and fabricated (Figure 5). The model includes a four-component balance integrated into the dual-strut mounting assembly. An array of combustion modules are embedded within the model along the full span, and the struts also include the tubing and wiring for the hydrogen and air supplies and the high voltage pulsed source. The model is designed to mount directly on the tunnel wall of the NASA Langley 0.5-m Supersonic Wind Tunnel. However, tunnel schedule constraints and extensive safety protocols precluded testing of this model during the period of performance of the current program.

Finally, the observations of the effectiveness of impulsive excitation introduce a new framework for understanding the dynamics of the control of flow separation. It is apparent from these results that the initial reattachment is dependent on the nature of the impulse or initial transient and **not** on the non-dimensional frequency. The frequency **is** critical in determining whether and when the flow will detach again. Thus, to keep a flow attached indefinitely, one does need to introduce perturbations at the right frequency relative to the time scales of the flow. However, ***to momentarily reattach a separated flow, an impulse is sufficient.*** Thus, one can think of separation control as an intricate balance between reattachment and separation in which reattachment dynamics are triggered in just the right manner so as to avoid the recurrence of separation.

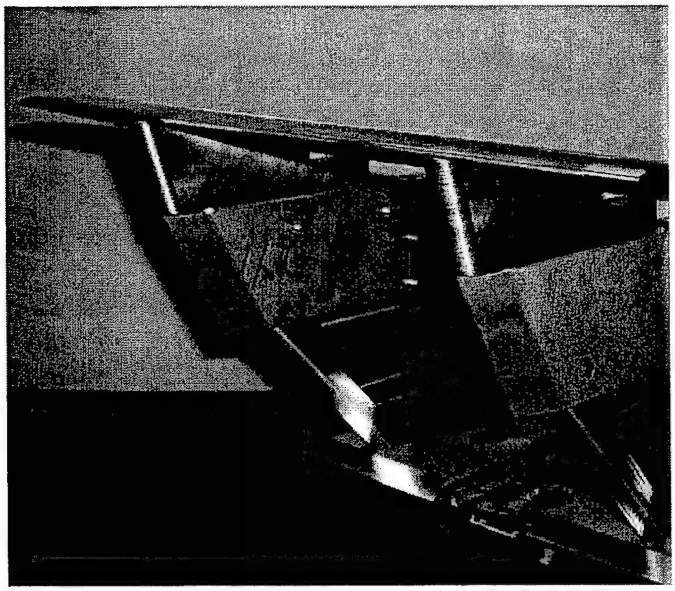

Figure 5. Picture of assembled transonic wing model with integrated combustion actuators across span. Support struts house tubing for fuel and air supply and an integrated set of load washers providing 4-degrees of measurement (lift, drag, pitch, roll). Base plate designed to fit hatch of NASA-Langley Supersonic Wind Tunnel.

3. MEMS Fabrication of Microjet Arrays

3.1 Background

The major portion of this program was devoted toward the development and characterization of aerodynamic control via combustion actuators as described in the previous section. That effort relied on conventional machining and assembly approaches to fabricate and integrate combustion actuators in the wing models. However, for the future viability of such technology on large numbers of low-cost UAVs, a simpler, batch fabrication approach is required for fabrication of these microjet arrays.

A single microjet combustor consists of four main components: fluidic channels for fuel handling, electrically conductive pathways for ignition, a cavity for combustion, and an exhaust port for jet formation. Figure 6 illustrates the basic layout of these components in a microjet combustor.

Fabrication of a single microjet combustor is feasible using conventional machining techniques. However, when multiple jets are needed and must be combined into an array, the conventional option becomes impractical. This is due largely to the difficulties with fabrication of the needed three-dimensional fluidic/electrical networks. The greatly increased processing times that result from the serial nature of conventional machining are also of concern. An alternative fabrication approach that addresses these problems is MEMS and microelectronic processing. The inherent batch processing of these techniques make them an attractive solution..

In addition to batch fabrication, MEMS processes enable substantially smaller features than conventional techniques. As a result, the main geometrical constraint of the array design is maintaining a sufficient chamber volume to support combustion. The MEMS processes do present one fabrication constraint important to microjet arrays. This is the planar construction of devices. In two dimensions, MEMS fabrication techniques allow significant design freedom in both size and geometry. However in the third dimension, normally thickness, size and geometry are severely restricted. As a result, devices typically have high aspect ratios and minimum

curvature in the direction of thickness. In microjet arrays this produces combustion chambers with an increased surface to volume ratio (S-V ratio). Additional surface area increases quenching within the chamber and increases the minimum required volume to maintain combustion. Previous work has examined this effect and the results applied to the design of these arrays.

3.2 Fabrication

The multi-layer design of many MEMS devices results from the planar nature of typical fabrication processes. A series of layers, one after the next, build up the final structure. Features added to a layer, either by removal or addition of material, are later covered by subsequent layers creating embedded structures. These features can be such things as channels, electrical wiring, cavities, etc. With careful design, the features can pass between layers enabling the fabrication of complex three-dimensional networks.

Earlier combustor experiments identified minimum chamber volumes appropriate for microjet arrays. The relatively thick array structures needed eliminates traditional thin film techniques as too slow or costly. However, the lamination approach long used in the fabrication of thick-film substrates is well suited for fabrication of the microjet arrays. Relatively thick sheets of material can be patterned separately and then stacked and bonded together to form a final device. Figure 7 demonstrates a three-layer design used to create a simple enclosed cavity. Sheets are patterned, aligned, and pressed together using alignment dies. This technique, like most planar processes, can create complex three-dimensional networks of channels.

The actual processing details of lamination are entirely material dependent. Selection of the material is important and, in the case of the microjet array, it must take into consideration the environment within the operating device. First, combustion creates significant local temperature rises and generates highly reactive byproducts. Second, the combustion events create high chamber pressures, cyclically stressing the device body. Finally, spark signals traveling within the array for ignition generate high electric fields and must be insulated to prevent arcing. Fortunately, these requirements are well satisfied by a number of ceramic materials. In the end a

high purity 99% Al_2O_3 ceramic was chosen. High purity alumina exhibits excellent mechanical stability and chemical inertness at high temperature. It maintains the high electrical breakdown strength needed for the spark electrodes. It is also readily available in many forms from commercial venders.

Thin brittle ceramic sheets are too fragile to be practical in device construction. As a result, alumina sheets used in lamination are unsintered or "green". These green sheets are a mixture of ceramic powder and organic binders that form a pliable material. This pliability in ceramic green tape is vital for microjet fabrication. Besides creating a pliable material resistant to fracture, the organic binder creates the initial low-temperature bond between the individual sheets during lamination.

Use of nonconductive alumina for the device body enables the embedding of spark electrodes directly in the housing. These electrodes are formed by screen-printing platinum ink on the ceramic green tape prior to lamination. Electrical pathways can pass between layers by addition of small vias filled with the conductive ink. Electrodes fabricated in this method are hermetically sealed within the device body and do not create additional pathways for gas flow. Selectively printing conductive pathways on multiple layers allows positioning of spark gaps on opposing walls that arc across the volume of the combustion chamber. Without this ability, spark gap electrodes would be required to share a wall. These arcs would travel along the surface of one wall, achieving less than optimum ignition.

Laser Machining

Prior to lamination, the green tape must be patterned to create channels and cavities in the finished device. There are a number of options for producing these patterns in green ceramic tape. Large scale manufacturers typically use dies to stamp the desired patterns. However, in an R&D environment with frequent design changes, dies are cost prohibitive. An alternative to die stamping is laser machining. Unlike mechanical cutting processes where material is sheared from the bulk, laser cutting involves ablation. The material absorbs the impinging beam energy and becomes superheated. This superheated material sublimates to a gas /plasma and is ejected

from the bulk in a self-clearing action (Figure 8). With proper adjustment of laser parameters, the resulting cut is debris-free.

The precision laser cutting system in use at Georgia Institute of Technology is a Resonetics Impressario Series unit (see Figure 9). This system is based around a solid-state 1047nm Nd:YLF pulsed laser that outputs 12 watts at the cutting head (1000Hz). Depending on cutting requirements, this system can be reconfigured to operate at a frequency doubled 523nm wavelength. The laser, optics, and cutting head are all fixed. Sample movement is handled by an x-y-micro-positioning stage that incorporates optical encoders and is accurate to ±0.1□m over its 300mm x 300mm travel. The cutting beam diameter is approximately 75□m using the 1047nm wavelength and 25□m while operating at the 523nm wavelength. Laser pulsing and movement of the positioning stage are controlled via computer interface. Design patterns are first generated in AutoCad™ and output in DXF format. The output file is loaded into the machining system where it is converted to the appropriate machine code. At the same time, all necessary machining parameters are applied (e.g. cutting speed, pulse rate, cutting order, etc.). Once the file is converted the sample is loaded and the entire cutting process is automated.

Lamination

Fabricating a microjet array with complex three-dimensional structures requires bonding multiple sheets of the ceramic tape (Figure 10). The first step in this process is sorting and stacking of the patterned green ceramic sheets. Next, the patterned sheets are aligned onto a die using alignment holes cut in the ceramic and alignment pins attached to the die. Once the sheets are situated in the bottom portion of the die, the die top-cover is added and the entire unit is inserted into a hydraulic press (Carver model #3851) with aluminum platens preheated to 75° C (Figure 11). Pressure is applied at 6Mpa (≈900psi) for 30 seconds. The combination of elevated temperature and pressure softens the binder system allowing the layers to temporarily bond. However, the window for temperature and pressure variations is relatively small. Excessive heat softens the binder allowing it to flow freely. This can lead to severe deformations in the device, effectively destroying it. Excessive pressure will induce the same device-damaging flow. After lamination the layers are weakly bonded to one another. This attachment is created solely from

binder system and does not involve the dispersed ceramic powder. To form the final monolithic device the binder system must be removed and bonds created between the ceramic particles.

Burnout and Sintering

Green ceramic tape remains in a pliable state until the organic binders are removed and the remaining grains of alumina powder are sintered. This removal and sintering is done through a two step heating process. The first low-temperature step slowly heats the material to a point where organic material either evaporates or decomposes. In the microjet alumina tape, the material is heated to 350° C at a rate of 0.50° C/min and maintained at that level for 4 hours. The slow ramp rate allows the generated gases to diffuse through the tape without damaging the device (e.g. voids, delamination, and fracture). Maximum ramp rate is ultimately controlled by the longest diffusion path within the device (e.g. thick structures require a slower ramp rate than thinner structures). It is also important to account for thermal generation in the decomposition of organics. Rapid ramp rates can lead to thermal runaway where the exothermic reaction of decomposition drives the internal sample temperature well above surrounding temperature increasing the effective heating rate. With careful control, samples with diffusion paths in excess of 5mm have gone through successful organic removal.

Once the organic binders have been removed the final heat treatment stage can occur. This final stage is a high temperature sintering. Individual particles of the ceramic powder bond together and densify into a monolithic structure. During this phase the sample is heated from 350° C to 1450° C at a rate of 3° C/min and held for 4 hours. Afterwards the device is cooled to room temperature at 10° C/min. An important byproduct of the densification is an isotropic shrinkage of 18% that must be considered when specifying dimensions in green tape patterns

3.3 Devices

Radial Array

An array of four microjets was fabricated using the previously discussed fabrication technique. The device consists of four combustion chambers with exhaust ports directed radially outward at 90° spacings. A stoichiometric fuel supply of propane/air premix is attached to a single inlet and

distributed to the individual chambers via a series of embedded channels. Cross-sectional area of the channels is well below the threshold necessary for sustained combustion. This allows for continuous fuel flow and results in a valve-free combustor design. Ignition is supplied by a network of embedded platinum spark electrodes. These electrodes are individually addressable allowing the selective firing of each jet. Figure 12 shows a layout of the individual layers prior to alignment and lamination. Figure 13 is an image of the finished array after lamination and sintering.

The radial array was connected to an external spark generator, supplied with the previously mentioned fuel, and tested. Images of an operating jet were recorded using a standard CCD camera with a single-pass Schlieren visualization system. Figure 14 demonstrates single chamber operation of this array with generation of a subsonic jet. Additionally, PIV data was obtained for the array and the results are shown in Figure 15. Four plots, taken at 0.5ms intervals, demonstrate typical jet formation with clear starting vortices that travel downstream following the jet development. Duration of the pulsed jet is slightly longer than one millisecond and the time-averaged measurements of peak jet velocity exceed 80 m/s. Note that this time averaging partially masks downstream turbulence in the PIV results.

Contoured Arrays for Airfoils – Nonplanar Lamination

Injecting a microjet into the airflow of typical airfoils requires incorporating the array into a region of the airfoil where the effect of disturbances is magnified. The result is a need for arrays that precisely mimic the profile, a profile that is normally curved. A fabrication challenge arises since lamination techniques typically result in devices with flat, planar surfaces. To obtain a contoured array two approaches were explored: nonplanar lamination and post-sinter shaping. The first approach induces curvature during the lamination step. Instead of pressing the sheets with flat dies (see Figure 11), a die set in the shape of the airfoil is used (see Figure 16). During lamination the array assembly conforms to the shape of the mold and results in an appropriate curvature that follows the airfoil profile. After lamination the array is sintered while supported by a similarly shaped refractory brick (see Figures 17, 18). The final device is a six-microjet array with the exhaust port directed normal to the array surface. Exterior array dimensions are 32mm x 44mm x 3.2mm and volume of each combustor chamber is approximately 0.08cc.

Propane/air premix is supplied by a single fuel inlet and distributed to each combustion chamber through a network of fluidic channels. Platinum spark electrodes embedded within the array housing supply a spark signal to each chamber allowing independent ignition. The faint outline of these embedded electrodes can be seen in Figure 19 due to the slight translucence of the alumina housing.

Contoured Arrays for Airfoils – Post Sinter Shaping

Previous work has indicated improved aerodynamic control when the exhaust jet is directed parallel to the fabrication plane, similar to the original radial array. Arrays with this port orientation create two fabrication difficulties. The first is shaping the port region of the device to the profile of the airfoil. With ports located on the assembly edge during lamination, shaped dies are not an option for producing a curved profile. The second fabrication difficulty is maintaining a uniform port cross-section during lamination. During the lamination and sintering processes, wide spans of unsupported material are likely to deform (see Figure 20). This undesirable deformation alters the final exhaust port geometry and dramatically affects jet performance.

An alternative fabrication approach has been developed which successfully addresses the difficulties of fabricating these appropriately contoured arrays with exhausts ports directed parallel to the surface. The technique consists of adding a sacrificial region to the ported end of the array (see Figure 21). This region supports the port openings during lamination and sintering when deformation is most likely to occur. After sintering, the sacrificial material is removed using a precision diamond grinder. The removal process exposes the buried exhaust ports and can accurately reproduce virtually any airfoil profile needed (Figure 22). One benefit of this design is that the bulk of the array can be embedded within the airfoil as desired. Only a small portion of the array requires exposure to the airstream – the ported edge (Figure 23). Embedding the main body of the array within the airfoil simplifies any necessary electrical and fuel connections. A finished array of three microjets and exhaust ports directed parallel to the surface is shown in Figure 24. The ported edge of this particular array is shaped to conform to a simple generic profile. External dimensions of the array are 40mm x 25mm x 4.3mm and the volume of the individual combustion chambers is approximately 0.19cc. As with the previous arrays, the

combustion chambers are all fueled from a single fuel inlet and the spark electrodes are individually addressable to allow selective firing of each chamber.

Interlinked Chambers

Finally, a novel approach involving interlinked chambers was developed to simplify the requirements for power electronics and spark electrodes. An additional flow passage is fabricated to allow some of the combustion product to travel from one chamber to an adjacent one. The combustion product ignites the premixed fuel/air mixture, obviating the need for a spark electrode and the associated electronics. In this way an array of several modules can be controlled by a single "pilot" chamber. A 14-actuator array demonstrating this concept is shown in Figure 25.

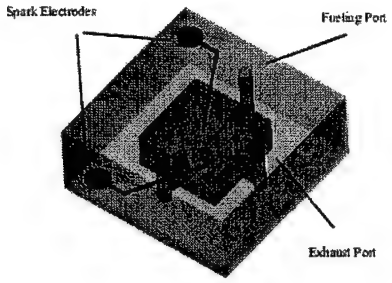

Figure 6. Layout of single microjet combustor.

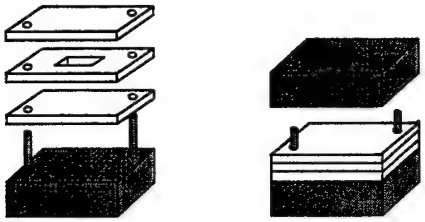

Figure 7. Alignment and bonding of 3-layer device.

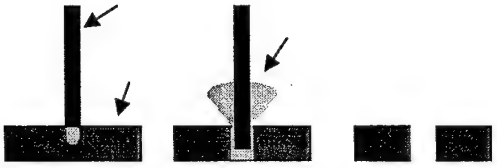

Figure 8. Steps in laser ablation.

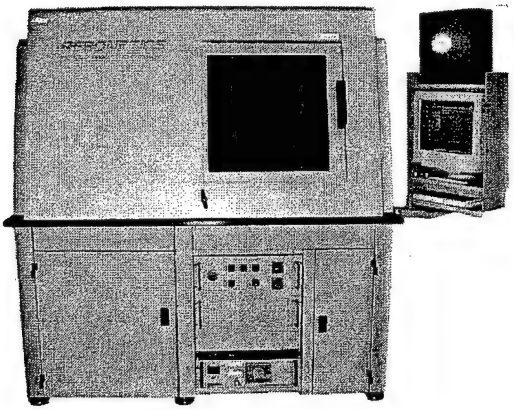

Figure 9. Resonetic's Nd:YLF laser micromaching system.

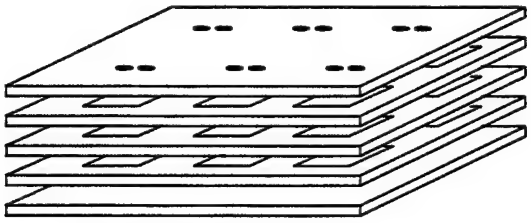

Figure 10. Initial stack of unbonded green sheets.

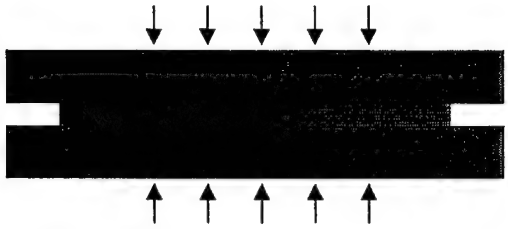

Figure 11. Lamination of sheets in press.

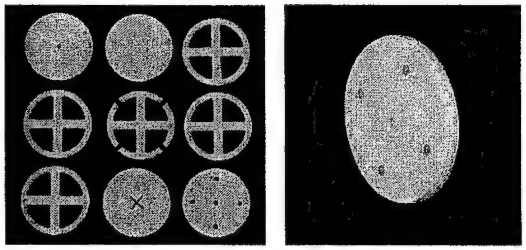

Figures 12 and 13. Layout of device layers before lamination and finished four-jet radial array.

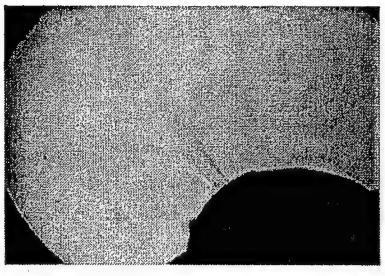

Figure 14. Schlieren image of radial array jet.

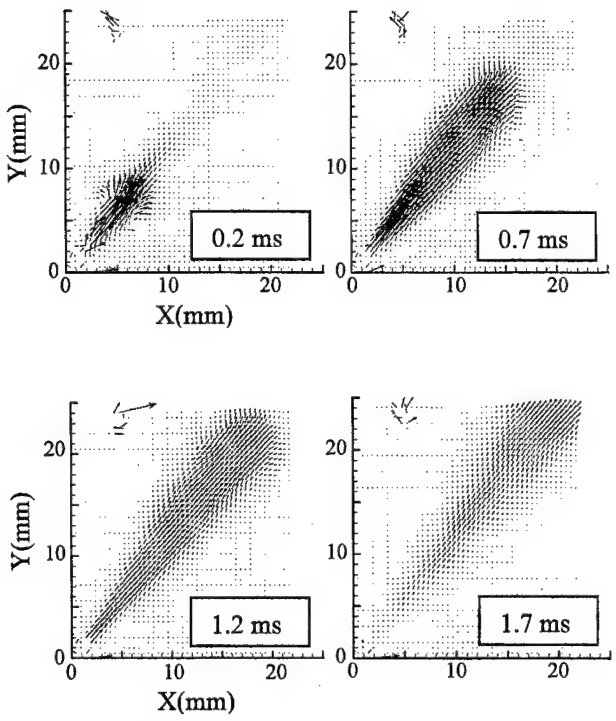

Figure 15. PIV measurements of radial array jet.

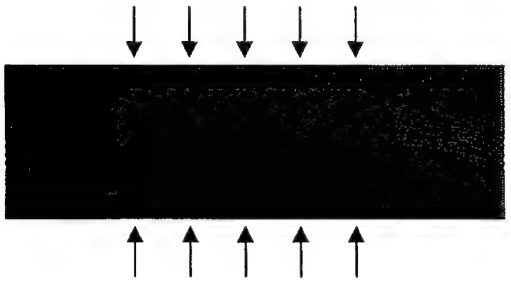

Figure 16. Non-planar lamination die.

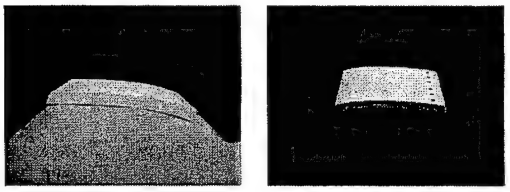

Figures 17 and 18. Molded array before and after sintering.

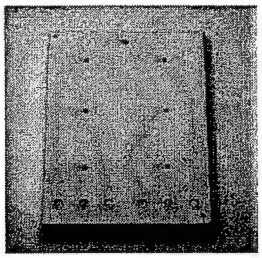

Figure 19. Top view of molded array (note the six embedded spark traces).

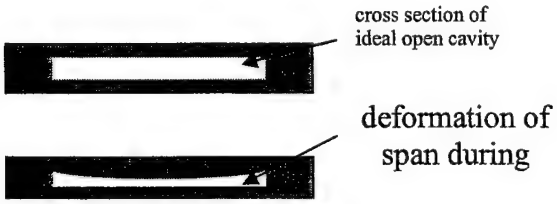

Figure 20. Deformation of unsupported cavities during lamination and sintering.

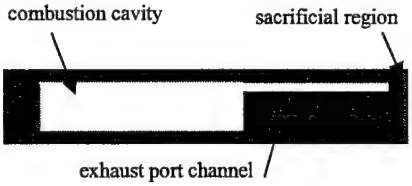

Figure 21. Cross-sectional representation of array fabricated with sacrificial region.

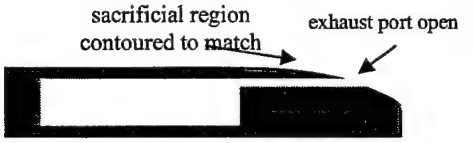

Figure 22. Cross-sectional representation of array after shaping exposes exhaust port.

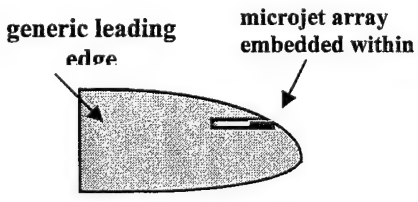

Figure 23. Array embedded in airfoil with only ported edge exposed to airflow.

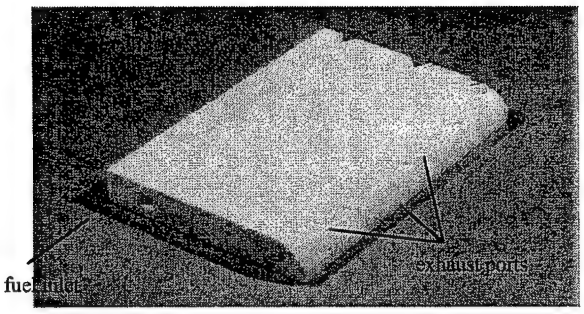

Figure 24. Microjet array with shaped leading edge (three jets).

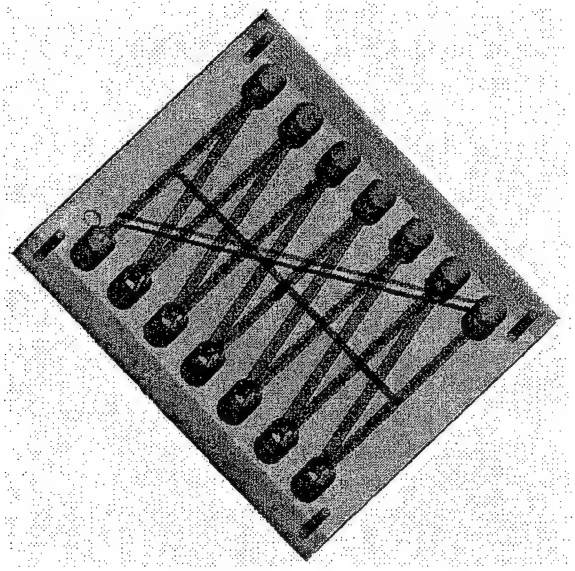

Figure 25. Rendering of 14-combustor array employing ignition conduits to link combustion chambers.

4. Concluding Remarks

The AVIA program achieved several key milestones in advancing active flow control technology, ranging from quantifying system level benefits for specific UAV platforms to significant milestones in actuator technology. Highlights of key flow control technology advances are noted below:

- ***Pulse Modulation of Synthetic Jet Waveform***–A major research discovery concerns the improvement of synthetic jet effectiveness through the pulse modulation of the sinusoidal excitation signal. Aerodynamic benefits, such as lift enhancement, are increased, and the actuator power required is decreased through a reduced duty cycle (see Parekh & Glezer [2000] and Glezer & Amitay [2002]).
- ***Micro Combustion-Driven Fluidic Actuators***–Small-scale modular combustion-driven actuators were invented and developed to address the need for high power actuation (Crittenden *et al.* [2001]). These devices produce an intense, short-duration (order 1ms), fluidic impulse whose periodicity is controlled by a spark ignition source in the combustion chamber (typically, 1 cc in volume). These devices can be integrated as an array to provide continuous control across the span of a wing and can be fed by a variety of fuels. For low-cost, bulk fabrication, a MEMS-based approach was developed, and several MEMS-fabricated arrays were produced.
- ***Impulse Control of Reattachment Dynamics***–Previous research on separation control had focused primarily on sinusoidal excitation of the separated shear layer to effect reattachment. Through the use of the combustion actuators, this research has shown that

a single pulse is adequate to reattach momentarily a separated flow. This result is consistent with the use of a pulse modulated sinusoidal waveform for the case of piezoelectric synthetic jet actuators. The transient response of the separated flow to excitation indicates that the reattachment dynamics are controlled primarily by the impulse not the frequency. Even a short 1-ms pulse can have a lasting aerodynamic effect over an order of magnitude longer time period (Funk *et al.* [2002]). The frequency of excitation, on the other hand, is critical to keeping the flow attached. The pulse must be repeated frequently enough to keep the flow from separating again. This approach is shown to be effective in delaying stall more than 10 degrees beyond the typical limit.

Some of the foundational results of this work, particularly with regard to implementation of piezoelectric synthetic jet actuators, are being advanced through a NASA-funded program on a full-scale, flying-wing shaped UAV. Initial wind tunnel results on a full-scale 3-D vehicle with synthetic jets at the leading edge are demonstrating significant pitch and roll authority at angles of attack for which the wing is partially stalled (Parekh *et al.* [2003] and Amitay *et al.* [2003]).

Future research should continue along several paths. First, additional work is needed to provide detailed characterization of the aerodynamic effects of combustion-driven actuators on 2-D and 3-D geometries in low-speed and transonic flow regimes. Second, the actuator technology should be advanced to include operation on liquid fuels in addition to the gaseous fuels demonstrated in this work. Third, an applied research and development program should be initiated to enable flight demonstration and technology transfer to Air Force applications.

Acknowledgements

The authors gratefully acknowledge the many insightful comments and keen suggestions provided by our technical monitors at AFOSR and DARPA throughout the course of this work. Without their encouragement and critical guidance this research would not have made such major strides in aerodynamic flow control innovations. These key individuals are Drs. Steve Walker, Tom Beutner, Rich Wlezien, and Jim McMichael. Dr. Steve Walker is the current DARPA MAFC program manager, succeeding Drs. Wlezien and McMichael. Dr. Tom Beutner is the current AFOSR technical monitor for this project.

Our colleagues at the School of Aerospace Engineering played a key role during Phase I of this program. Professor Tony Calise developed the foundation for adaptive neural-net-based controls applicable to this type of actuation. Professor Dimitri Mavris and Dr. Dan DeLaurentis conducted system studies to provide technology impact forecasts for the flow control technology being developed. At the Georgia Tech Research Institute, Dr. Michael Amitay, assisted by Mr. Shayne Kondor and Mr. Steve Williams, made important early contributions to the wind tunnel investigations involving piezoelectric synthetic jets. Mr. Joe Hurst and Mr. Duane Patterson provided the engineering expertise to develop customized power electronics for both the combustion and piezoelectric actuators.

Finally, this work would not have been possible without the partnership of our colleagues at the Boeing Company and Metacomp Technologies. At Boeing Phantom Works in St. Louis, MO, Mr. Brad Osborne and Mr. Pat O'Neill led the project efforts devoted to system studies of both a generic tactical UAV and the X-45A. Mr. Bill Butters developed the Model 1301 UAV test vehicle that was made available by Boeing for use during the early stages of this program. Drs. Val Kibens and Bill Bowers, Technical Fellows at the Boeing Company, helped shape the direction of the overall program and provided a key linkage to the active flow control research programs within Boeing. At Metacomp Technologies in Westlake Village, CA, Drs. Palaniswamy, Goldberg, and Chakravarthy conducted the computational fluid dynamics analysis that was instrumental in confirming the high frequency transient phenomena observed experimentally in low-speed separation control studies and in providing preliminary estimates of transonic performance of the combustion actuator technology.

References

1. Amitay, M., Washburn, A. E., Anders, S. G., Parekh, D. E., Glezer, A., 2003, "Active Flow Control on the STINGRAY UAV: Transient Behavior," AIAA Paper 2003-4001.

2. Amitay, M., Glezer, A., 2003, "Controlled Transients of Flow Reattachment over Stalled Airfoils," *International Journal of Heat Transfer and Fluid Flow*, Vol. 23, No. 5, pp. 690-699.

3. Idan, M., Calise, A. J., Kutai, A. T., Parekh, D. E., 2003, "Adaptive Neural Network Based Approach for Active Flow Control," in *Manipulation and Control of Jets in Crossflow*, edited by Karagozian, A. R., Cortelezzi, L., and Soldati, A., published by Springer Wien New York, pp. 287-297.

4. Crittenden, T., 2003, "Fluidic Actuators for High-Speed Flow Control," PhD Thesis, Georgia Institute of Technology.

5. Crittenden, T., Glezer, A., Funk, R., and Parekh, D., 2001, "Combustion-Driven Jet Actuators for Flow Control," AIAA Paper 2001-2768.

6. Funk, R., Parekh, D., Crittenden, T., Glezer, A., 2002, "Transient Separation Control Using Pulse Combustion Actuation," AIAA Paper 2002-3166.

7. Glezer, A., and Amitay, M., 2002, "Synthetic Jets," *Annual Review of Fluid Mechanics*, Vol. **34**, pp. 503-529.

8. Parekh, D., and Glezer, A., 2000, "AVIA: Adaptive Virtual Aerosurface," AIAA Paper 2000-2474.

9. Parekh, D., Palaniswamy, S., and Goldberg, U., 2002, "Numerical Simulation of Separation Control via Synthetic Jets," AIAA Paper 2002-3167.

10. Parekh, D. E., Williams, S. P., Amitay, M., Glezer, A., Washburn, A. E., Gregory, I. M., Scott, R. C., 2003, "Active Flow Control on the STINGRAY UAV: Aerodynamic Forces and Moments," AIAA Paper 2003-4002.

Appendix

Combustion-Driven Jet Actuators

(Chapter 3 excerpt from Crittenden, T., 2003, "Fluidic Actuators for High-Speed Flow Control," PhD Thesis, Georgia Institute of Technology, pp. 41-88 [text] and 137-159 [figures])